The Performance of Cu(In,Ga)Se_2-Based Solar Cells in Conventional and Concentrator Applications

J.R. Tuttle, J.S. Ward, A. Duda, T.A. Berens, M.A. Contreras, K.R. Ramanathan, A.L. Tennant, J. Keane, E.D. Cole*, K. Emery, and R. Noufi

National Renewable Energy Laboratory, Golden, Colorado USA
(ph) 303-384-6534, (fax) 303-384-6430 (e-mail) john_tuttle@nrel.gov

*CoGen Solar, L.L.C., Centreville, Virginia USA
(ph) 703-266-0798, (fax) 703-266-0798 (e-mail) CoGenSolar@aol.com

ABSTRACT

Cu(In,Ga)Se_2 (CIGS) solar cells are under investigation for 1-sun and concentrator applications. Design criteria are examined and reveal that only grid design modifications are required. In the special case where cell width dimensions are 4-5 cm, an interdigitated design removes the back contact as a loss mechanism. Processing issues relating to the intrinsic ZnO layer are critical to optimal and reproducible cell performance. 1-sun and 20 sun performance of 17.7% are reported for different cells. The latter represents a 2.9% absolute improvement over the 1-sun control measurement. 20% performance is therefore a realistic goal. CIGS-based cells represent a viable concentrator technology.

INTRODUCTION

In 1996, an examination of the photovoltaics (PV) arena reveals a downturn in federal R&D while production and market growth are on the upswing. This scenario presents a unique backdrop to the investigation of novel directions in solar cell development. One such direction is the application of polycrystalline thin-film PV technologies to concentrator designs. Historically, concentration designs have been applied to high-efficiency, high-cost crystalline technologies as a means to boost the module total (W/m^2) and specific (W/Kg) power for space applications [1], and to reduce total module cost ($/W) for terrestrial power generation. Concentration ratio's ranging from 6-500 [2-4] are typical and serve to offset the high cell cost with lower balance-of-module costs. Opponents of this approach point to the high additional balance-of-system (BOS) costs associated with mechanical support structures and accurate ($\pm$ 1°) tracking systems, and the sensitivity of concentrator systems to reductions in direct radiation.

One possible way to short circuit the argument is to use low-cost, moderate efficiency solar cells in the concentrator configuration. Thin-film Cu(In,Ga)Se_2(CIGS)-based cells represent such a technology. Laboratory cell performance of 17.7% (total-area) is rapidly closing the gap with Si-based technologies at lower projected manufacturing costs [5,6]. Our first effort at CIGS concentrator cells produced a 17.2% device at 22 suns. This represented a 2.1% absolute improvement over the 15.1% 1-sun control [7]. It is the intent of this work to match the previously observed improvement with our present state-of-the-art 1-sun cells to see performance under low-level concentration ($\approx$ 20 suns) of near 20%.

Mat. Res. Soc. Symp. Proc. Vol. 426 © 1996 Materials Research Society

In this contribution, our path to this goal is charted. We begin with the basic CIGS device design considerations in going from 1-sun to 22-sun illumination levels. Data pertaining to a 17.7% total-area, 1-sun performance level is presented. For the purpose of demonstration, small-area (0.1-cm^2) concentrator devices are fabricated and tested. Concurrently, a design for a cell with dimensions compatible with ENTECH's linear concentrator has been pursued. The primary consideration in these designs is lateral conduction losses in the Mo back electrode. The concern is that exposure of the Mo film to Se reduces its lateral conductivity considerably relative to its bulk value. To address this, an "interdigitated" back-contact design is presented.

DESIGN CONSIDERATIONS

1-Sun

A schematic for the standard 1-sun CIGS-based solar cell is shown in Fig. 1. The salient features of this device include a "thermally" thick, insulating soda-lime glass substrate, a sputtered Mo back contact whose thickness and structure influence its secondary role as a conduit for impurity migration from the glass to the absorber, and a sputtered ZnO emitter.

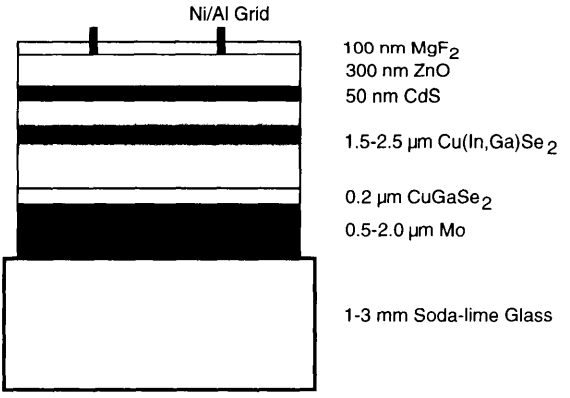

Fig. 1 Schematic of CIGS-based solar cell.

In Fig. 1 (not to scale), a 3μm thick Ni/Al grid is shown. The design of this grid has been accomplished using modeling code that sums the individual power loss elements including grid shadowing and lumped series resistance [8]. In Fig. 2, an example of such an effort is shown for a 1.125-cm^2 grid structure created for our devices. The code balances resistive losses against optical (shadowing) losses. The optimum design produces a minimum power loss of 6.95%. This does not include other losses external to the junction such as reflection from the emitter surface. In this example, the clear choice for further optimization is in the finger resistance. Increasing the thickness to 6.0 μm reduces the total power losses to 5.11%. There are additional loss elements that are not mentioned here that have been considered. They include bulk resistivities of the cell elements and the Mo/absorber contact resistance. These do not contribute much to the resistive losses because the cross-section for current transport is the entire cell area. Lateral transport in the Mo is also not an issue for small-area 1-sun devices. We will describe below how this element becomes significant under concentration.

Concentration

To operate the device under concentration, a first glance indicates the emitter and finger resistance elements may become factors. Additionally, lateral transport within the Mo is now considered. An In contact is made to the device around the perimeter, requiring a minimum transport distance of one-half the narrowest cell dimension. It is expected that

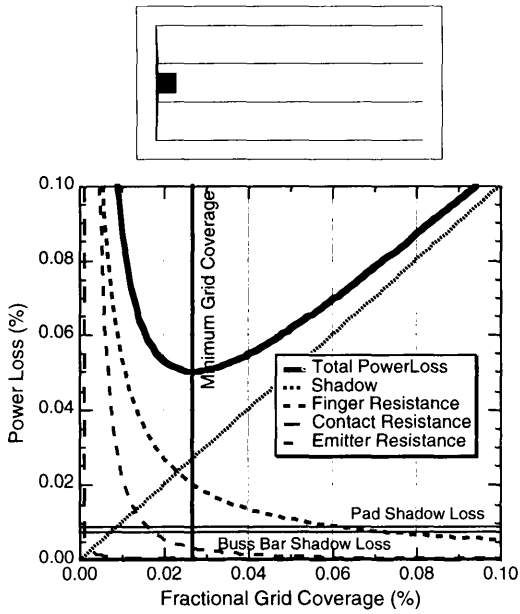

CIGS - 1 Sun

Input Parameters	Value
Metal Thickness:	3.00 μ
Metal Resistance:	4.00e-06 Ω-cm
Mimimum Line Width:	5.0e-03 cm
Contact Resistance:	1.0e-04 Ω-cm^2
Emitter Sheet Resistance:	20 Ω/sq
BC Sheet Resistance:	0.10 Ω/sq
Width Parallel to Fingers:	1.50 cm
Device Length:	0.75 cm
Short Circuit Current:	35.00 mA/cm^2
Open Circuit Voltage:	650.00 mV

Output Parameters	Value
Total Device Area:	1.125 cm^2
Buss Bar Area:	0.010 cm^2
Finger Area:	0.026 cm^2
Minimum Power Loss:	5.02 %
Finger Shadow Loss:	2.33 %
Buss Shadow Loss:	0.88 %
Pad Shadow Loss:	0.89 %
Total Shadow Loss:	4.10 %
Contact Resistance Loss:	0.02 %
Finger Resistance Loss:	1.99 %
BussBar Resistance Loss:	0.50 %
BC Resistance Loss:	0.03 %
Emitter Resistance Loss:	0.31 %
Total Resistive Loss:	2.85 %
Total Power Loss:	**6.95 %**
Natural Finger Spacing:	0.188 cm
Natural # Fingers:	4

Fig. 2 Modeling effort for 1-sun illumination illustrating relationship between physical device parameters and associated resistance and shadow losses

lateral transport is affected by the inherent anisotropy of the Mo film conductivity. A further complication arises with the knowledge that the Mo free-surfaces contain Se, possibly in the form of a Mo_xSe. Unexpectedly, the sheet resistivity of the Mo (R_{mbc}) is measured to be 0.1 Ω/sq before and after exposure to Se at 600 °C. For the purposes of demonstration, we have initially used a grid pattern previously tested on GaInP/GaAs concentrator cells for operation at 100-200 suns [9]. This pattern is shown in Fig. 3. When we model this design for operation at 22 suns with a CIGS thin-film cell, we find that the limiting elements are the shadow and series resistance losses from the finger elements (Fig. 3). The design is optimized with 6 fingers and the available grid pattern starts with 8. Any additional grid lines (numbering 11 and 16, Fig. 3) serve only to increase shadowing losses. The electroplated Ni grid metallization used in this device also presents a significant loss element. The bulk resistivity of the contact is about 7x that of an evaporated Ni/Al contact used for 1-sun devices. We will improve on this in future work by using a lift-off technique for evaporated metal. Other critical features of this design are; the buss-bar area is not considered a shadow loss in a concentrator because it is outside of the illuminated area, and the back contact contributes less than a 0.1% power loss from the effect described earlier. It is still necessary to minimize the buss area as it contributes to dark junction current and subsequent losses in the open-circuit voltage (V_{oc}). As the photocurrent (J_{ph}) increases with concentration, this parasitic effect becomes minimal.

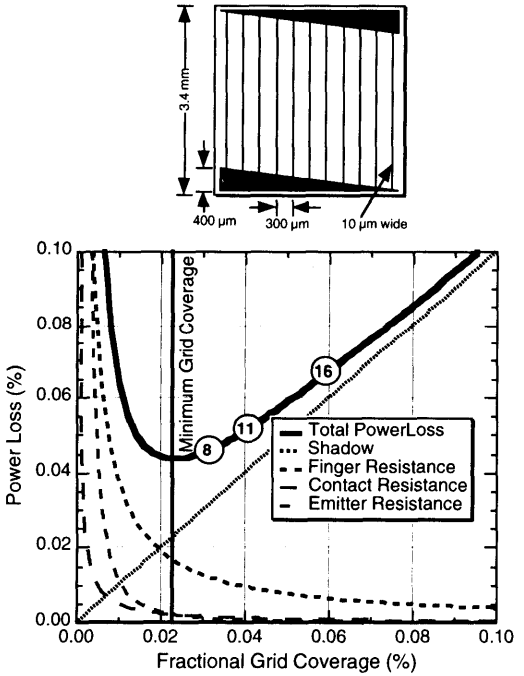

CIGS - 22 Sun

Input Parameters	Value
Metal Thickness:	8.00 μ
Metal Resistance:	3.50e-05 Ω-cm
Mimimum Line Width:	1.2e-03 cm
Contact Resistance:	1.0e-04 Ω-cm^2
Emitter Sheet Resistance:	10 Ω/sq
BC Sheet Resistance:	0.10 Ω/sq
Width Parallel to Fingers:	0.17 cm
Device Length:	0.33 cm
Short Circuit Current:	700.00 mA/cm^2
Open Circuit Voltage:	750.00 mV

Output Parameters	Value
Total Device Area:	0.055 cm^2
Buss Bar Area:	0.007 cm^2
Finger Area:	0.001 cm^2
Minimum Power Loss:	4.37 %
Finger Shadow Loss:	1.46 %
Buss Shadow Loss:	0.00 %
Pad Shadow Loss:	0.00 %
Total Shadow Loss:	1.46 %
Contact Resistance Loss:	0.21 %
Finger Resistance Loss:	1.65 %
BussBar Resistance Loss:	1.93 %
BC Resistance Loss:	0.02 %
Emitter Resistance Loss:	0.21 %
Total Resistive Loss:	4.02 %
Total Power Loss:	**5.48 %**
Natural Finger Spacing:	0.055 cm
Natural # Fingers:	6

Fig. 3 Modeling effort for 22-sun illumination illustrating relationship between physical device parameters and associated resistance and shadow losses

In order for the CIGS-based cell to be compatible with the ENTECH linear-focusing concentrator, the cell dimensions require some modification. ENTECH's present Si cells are 4.83 cm x 9.65 cm, the former dimension being the width of the illuminated area. This would be twice the minimum distance current would have to travel in the Mo back contact to reach a bussbar outside of the illuminated area were no design modifications accomplished. This results in a singular power loss element of over 10% at 22-suns. This is clearly unsatisfactory. To address this shortcoming, an "interdigitated" contact was designed (Fig. 4). In this approach, 250 μm via's are etched through the cell to the Mo and a ≈10 μm x 150 μm Ni/Al grid is deposited by a lift-off technique. A grid of similar dimensions is then applied to the ZnO emitter to complete the interconnect. At this stage, there is approximately 30-50% of the cell inactive. A newly designed ENTECH prismatic cover is subsequently applied to redirect the illumination into the active cell regions.

The electrical and optical losses of this cell are modeled in a similar manner as before with the exception that shadowing by the grid is replaced with an added reflection loss off of the prismatic cover. With the large grid coverage and short transverse conduction lengths, all losses decrease to near zero with the exception of finger resistance losses. For a 10 μm evaporated Ni/Al grid, the resistive loss from the fingers is between 5-6%.

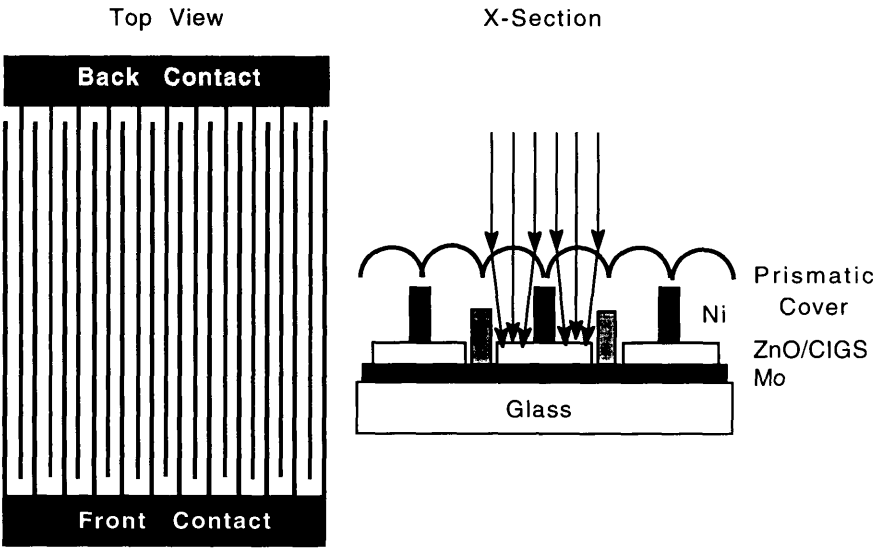

Fig. 4 Schematic illustration of interdigitated device design to minimize back contact series resistance losses

EXPERIMENTAL

CIGS thin-film absorbers are fabricated by physical vapor deposition of the elements onto a heated substrate of Mo-coated soda-lime glass. The absorber is deposited in several stages. First, 2000 Å of a near-stoichiometric layer of $CuGaSe_2$ (CGS) is deposited at 350°C. The composition of the layer is designed to minimize the out/in-diffusion of Ga/In into the bulk to control the composition of the CIGS. The CIGS is deposited by a two-stage process described in detail elsewhere [10]. The absorber deposition is finished in such a manner as to enhance the formation of (In,Ga)-rich surface phases.

The CdS layer is deposited by chemical bath deposition CBD. The ZnO is deposited in two layers by RF sputtering. The high-resistivity layer of undoped ZnO is sputtered in a partial pressure of O_2 to a thickness of 50 nm. The conductive layer of Al-doped ZnO is sputtered to a thickness of 300 nm and 550 nm for 1-sun and 22-sun applications, respectively. The final sheet resistivity of the bilayer ZnO is 10-25 Ω/sq. Next, 3.0-μm Ni/Al grids with ≈ 3% obscuration are evaporated on 1-sun devices followed by a 100-nm MgF_2 anti-reflection coating. For concentrator devices, we have utilized grid patterns defined by standard photolithography (Fig. 3). The grid is constructed of 8 μm electroplated Ni for the small-area demonstration device. This device is completed by adding a MgF_2 anti-reflection coating. Contacts are made to the two front-contact bus bars, and to the Mo back contact via an In buss-bar that surrounds the cell.

Quantum efficiency (QE) measurements are performed in the dark in the wavelength range 380-1200 nm. Current-voltage (J-V) analysis was performed on the National Renewable Energy Laboratory's (NREL) ORC and X-25 solar simulators. Efficiencies

reported here for AM1.5 and concentrator configurations are referenced to either the global (ASTM E 892-87) or direct (ASTM E 891-87) spectra, respectively, at an irradiance of 1000 W/m^2. All measurements are performed at an approximate junction temperature of 25°C. Under concentrated illumination where thermal loading occurs, this requires cooling of the substrate. For cells deposited on 1-mm soda-lime glass, the thermal gradient across the substrate can be significant. At 20-suns, the chuck upon which the cell is placed for measurement must be held at 0 to -5 °C to maintain a junction temperature, and hence open-circuit voltage (V_{oc}), consistent with standard reporting temperature conditions of 25°C.

RESULTS AND DISCUSSION

1-Sun

In Fig. 5, the latest high-efficiency 1-sun result is presented. The improvement in performance relative to the previous 17.1% record device is observed in the V_{oc}. There is a slight shift in the absorber bandedge to higher energies which could account for the voltage increase. The current is maintained at 34.0 mA/cm^2 through an improvement in the blue response of the cell. The origin of this shift is either due to reduced recombination in the CBD CdS or a reduced thickness of the CdS layer. Power losses related to current generation and collection are indicated in Fig. 5. Further optimization can occur with reductions in the ZnO and CdS absorption losses.

Concentration

In a well-behaved cell operated under concentration, the V_{oc} will increase as $(AkT/q)\ln(J_{conc}/J_{1\text{-}sun})$, the short-circuit current (J_{conc}) linearly with concentration, and the FF with the voltage until other factors come into play. With the hope of improving on our previous best result of 17.2%, other absorber sections from the record device (run S773) were submitted for concentrator device fabrication. The ZnO thickness was increased to ≈ 6000 Å in order to reduce the sheet resistivity to 10 Ω/sq. Initially, our results did not contribute to the formation of a superior device. The results suggest a critical sensitivity of the device performance to the deposition conditions and subsequent quality of the sputtered 500Å intrinsic ZnO layer. In Fig. 6, current-voltage (J-V) curves representative of this effect are shown. The effect observed in curves (a) and (b) is referred to as "rollover" in the power quadrant, the white-light "kink" effect, or double-diode behavior. The diode phenomenon has been modeled [11] and the behavior attributed to interface states between the CdS and i-ZnO layers. The origin of the interface states is possibly related to sputter damage to the CdS surface and/or sensitivity of the CdS and ZnO to O_x in the plasma. The effect is air sensitive ((a) -> (b)), vacuum sensitive ((b) -> (c)), and illumination dependent ((c) -> (d)). Though the device partially recovered under concentration, the effect hampered its ultimate performance through reductions in current and fill-factor.

A second attempt was made with this absorber whereby another section that had been processed and exhibited the anomalous behavior described above was reworked. This is accomplished by stripping the grids, ZnO, and CdS in a 1:10 $HCl:H_2O$ solution, and

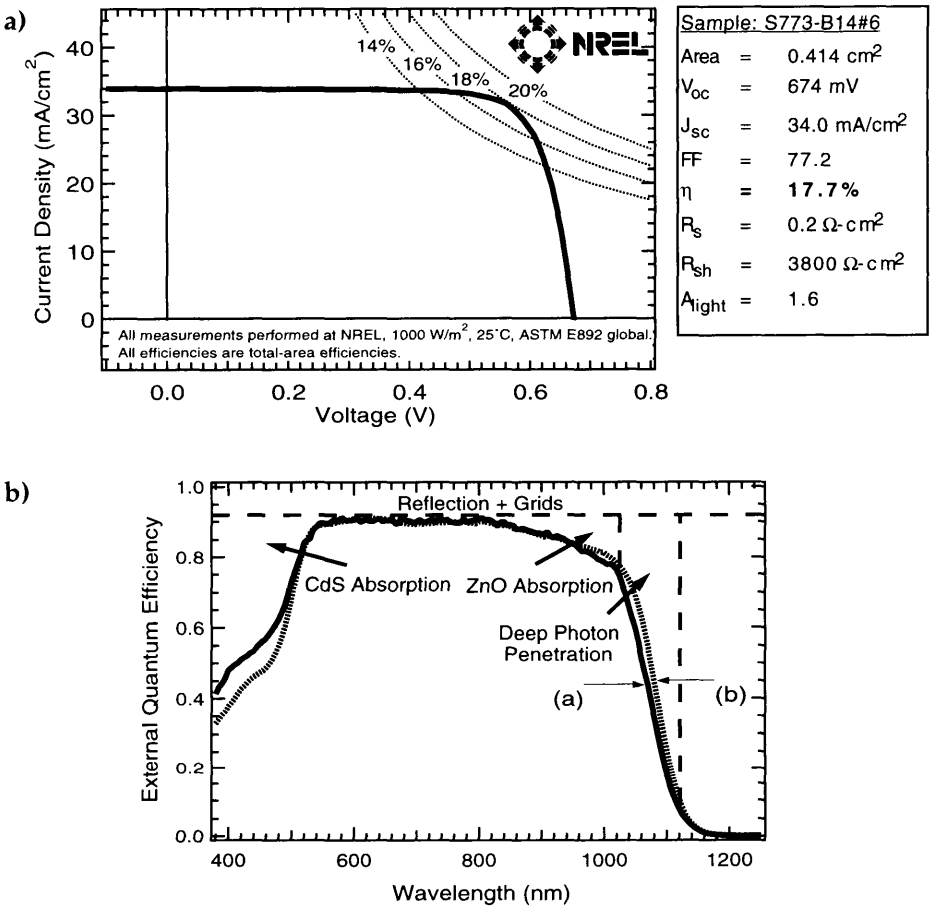

Fig. 5 J-V (a) and QE (b) measurements of high-efficiency CIGS-based cell. Current loss mechanisms are illustrated in (b).

redepositing the CdS and ZnO as before. In this rework effort, improved control and a reduced thickness (3500Å) of the ZnO was targeted. The result is shown in Fig. 7 - an obviously superior device to that of Fig. 6. This device was subsequently measured at 20-sun illumination and demonstrated 17.7% performance. This represents a 2.9% absolute improvement over the 1-sun control of 14.8%. The salient features of this device are the improved current at 1-sun due to the improved and thinner ZnO, the improvement of a 77% fill-factor to 79% under concentration, and a voltage increase of 101 mV. The improvement in FF suggests minimal series resistance losses at this level of concentration. This voltage increase is consistent with an diode factor of 1.30. Clearly, we did not reach our milestone of 20% due to the reduced 1-sun voltage of the concentrator cell relative to the 1-sun voltage of 674 mV reported for the record device. Likewise, the

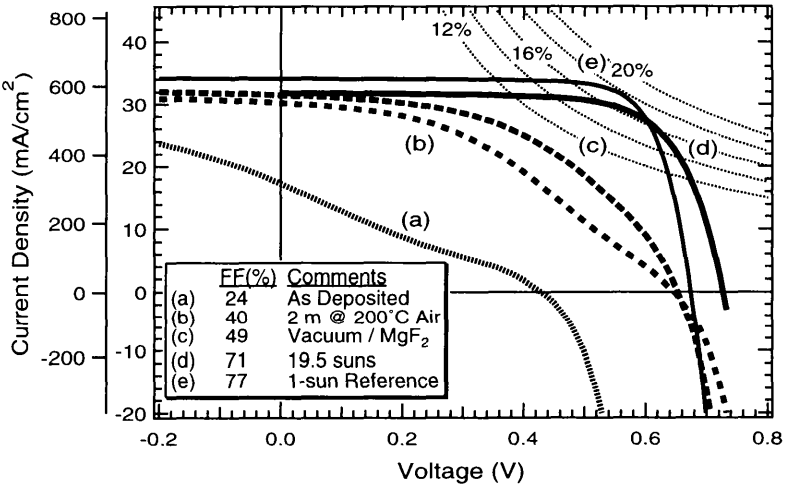

Fig. 6 J-V measurements for device designed for concentrator operation. (e) is 17.7% 1-sun device added for reference.

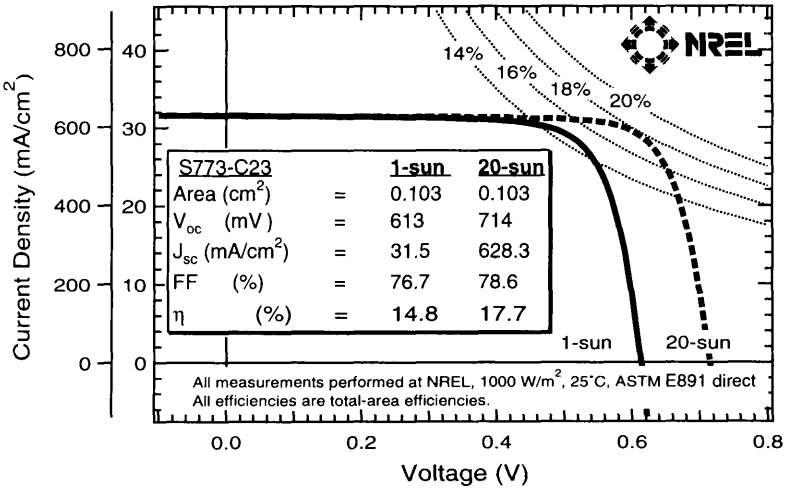

Fig. 7 J-V measurements for device operated at 1-sun and 20-sun direct spectrum illumination.

1-sun direct current is low relative to the achievable value. The most important lesson learned is that the reproducibility of the ZnO process may be as critical a challenge as that of the absorber process. The results also point to the positive effects of illumination on non-optimal devices. This is a benefit when considering cell and module reliability and lifetime issues in the field.

FINAL REMARKS

The product of this work is two new cell efficiency benchmarks: 17.7% 1-sun and 22-sun performance. At first glance, there would appear to be no benefit to concentration. To the contrary, this data supports further investigation. Clearly, performance superior to 17.7% is attainable. Additionally, the commercial application of this technology reduces material requirements 20-fold. New cell and module designs can capitalize on this by miniaturizing the concentrator hardware. It therefore becomes very probable that a cost-effective, thin-film, concentrator PV technology is achievable and viable.

ACKNOWLEDGEMENTS

The authors thank J. Dolan for technical assistance. This work was supported by NREL under Contract No. DE-AC36-83CH10093 to the U.S. Department of Energy.

REFERENCES

1. M.F. Piszczor Jr., M.J. O'Neill, and L.M. Fraas, Proceedings of the 23rd IEEE Photovoltaic Specialists Conference, 10-14 May, 1993, Louisville, KY (IEEE, New York, 1993) p. 1386.
2. N. Kaminar, J. McEntee, P. Stark, L. Adkins, B. Lapson, and D. Curchod, Proceedings of the 23rd IEEE Photovoltaic Specialists Conference, 10-14 May, 1993, Louisville, KY (IEEE, New York, 1993) p. 1213
3. M.J. O'Neill and A.J. McDanal, Proceedings of 13th NREL Photovoltaic Program Review, edited by H. Ullal and C.E. Witt (AIP Conf. Proc. **353**, New York, 1996) p. 621.
4. S. Yoon and V. Garboushian, Proceedings of the 1st World Conference on Photovoltaic Energy Conversion, 5-9 Dec., 1994, Waikoloa, HI (IEEE, New York, 1993) p. 1500.
5. K. Zweibel, Prog. in PV, **3**(5), 279 (1995).
6. V.K. Kapur and B.M. Basol, Proceedings of the 22nd IEEE Photovoltaic Specialists Conference, 7-11 Oct., 1993, Las Vegas, NV (IEEE, New York, 1992) p. 23.
7. J.R. Tuttle, M.A. Contreras, J.S. Ward, A.M. Gabor, K.R. Ramanathan, A.L. Tennant, L. Wang, J. Keane, and R. Noufi, Proceedings of the 1st World Conference on Photovoltaic Energy Conversion, 5-9 Dec., 1994, Waikoloa, HI (IEEE, New York, 1993) p. 1942.
8. T.A. Gessert and T.J. Coutts, J. Vac Sci. Technol. A., **10**(4), Jul/Aug 1992, p. 2013.
9. D.J. Friedman, K.A. Bertness, S.R. Kurtz, C. Kramer, A.E. Kibbler, and J.M. Olson, Proceedings of 13th NREL Photovoltaic Program Review, edited by H. Ullal and C.E. Witt (AIP Conf. Proc. **353**, New York, 1996) p.150.
10. J.R. Tuttle, A.M. Gabor, M.A. Contreras, A.L. Tennant, K.R. Ramanathan, A. Franz, R. Matson, and R. Noufi, Proceedings of the 1st World Conference on Photovoltaic Energy Conversion, 5-9 Dec., 1994, Waikoloa, HI (IEEE, New York, 1993) p. 47.
11. Y.J. Lee and J.L. Gray, Proceedings of the 1st World Conference on Photovoltaic Energy Conversion, 5-9 Dec., 1994, Waikoloa, HI (IEEE, New York, 1993) p. 287.